Pergamon

Journal of Structural Geology, Vol. 16, No. 9, pp. 1205 to 1215, 1994

0191-8141/94 $07.00+0.00

0191-8141(93)E0025-G

Structures in natural serpentinite gouges

EILARD H. HOOGERDUIJN STRATING* and REINOUD L. M. VISSERS

Department of Geology, Institute of Earth Sciences, P.O. Box 80021, 3508 TA Utrecht, The Netherlands

(*Received* 25 *May* 1993; *accepted in revised form* 24 *November* 1993)

Abstract—Serpentinite gouges from cataclastic fault zones in the Voltri Massif (NW Italy) are dominated by few discrete, boundary-parallel (Y) shears and oblique synthetic Riedel (R_1) shears separating domains of massive gouge. Unlike natural clay-rich fault gouges, the cohesive microbreccia domains only rarely show foliations. These structures dominated by discrete shears indicate a significant degree of localization of the deformation at the scale of the gouge. The dominant gouge-forming mechanisms were fracturing of olivine and pyroxene grains along (serpentinized) grain boundaries, and initiation of transgranular fractures in pyroxene grains in domains of lattice bending and grain indentation. Syn-tectonic serpentinization added to the weakening of fragments. Textural similarities with experimentally formed gouges suggest that the Voltri fault zones were dominated by stick–slip sliding, hence that they may represent fossil seismogenic faults. A notable aspect of the gouge texture in the Voltri fault zones is a sigmoidal shape of the Riedel shears which bend into parallelism with the Y shears. It is argued that this geometry was largely controlled by local perturbations of the stress field near heterogeneities on Y or P shears. The average spacing between the R_1 shears increases linearly with 0.47 times the distance between bounding Y shears. This proportionality may reflect a balance between the cohesive strength of the gouge material and the shear stresses acting on the bounding slip planes.

INTRODUCTION

AN IMPORTANT objective in modern structural analysis of thrust belts and extensional terrains is to assess the sense of movement on faults and shear zones. Field and experimental studies have shown that the most reliable kinematic indicators in brittle fault rocks are the sense of deflection of foliations (S) or synthetic P shears near their intersection with synthetic Riedel (R_1) shears, the obliquity of R_1 shears with respect to boundary parallel faults (Y shears), and the sense of offset of Y shears by R_1 shears (Fig. 1) (e.g. Logan *et al.* 1979, Rutter *et al.* 1986 and references therein). All of these structures are very common in clay-rich gouges and have been extensively studied (e.g. Riedel 1929, Skempton 1966, Tchalenko 1970, Logan *et al.* 1979, Chester *et al.* 1985, Rutter *et al.* 1986, Chester & Logan 1987, Evans 1988, 1990, Tanaka 1992). However, experimental work on quartz (Byerlee *et al.* 1978, Power & Tullis 1989) and quartz–montmorillonite gouges (Logan & Rauenzahn 1987) shows that foliations and P shears may not develop in clay-poor gouges, and that the smallest macroscopically visible fractures in such compositions may be closely spaced R_1 shears. The orientation of these R_1 shears is opposite to that of the sigmoidal foliations and P shears developed in clay-rich gouges, but their geometry may be virtually identical. This geometric similarity is further accentuated by the fact that R_1 shears may also have a sigmoidal shape. This imposes an ambiguity in the interpretation of brittle fabrics developed in natural clay-poor gouges, especially if there are no offset markers to confirm the movement sense on the gouge. Such ambiguity invites a study into possible kinematic reasons for the sigmoidal geometry of the R_1 shears as well as into simple geometric rules, if any, to discriminate between closely spaced Riedel shears and gouge foliations or P shears.

There is no unique relationship between the type of gouge fabric and gouge composition. This is clearly demonstrated in experiments on, for example, illite gouge (Moore *et al.* 1989) showing that not only the clay content but also the deformation conditions may influ-

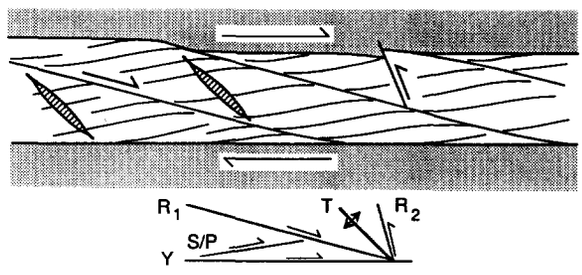

Fig. 1. Diagram showing geometrical relationships between the most common planar discontinuities in fault gouges. Synthetic (R_1) Riedel shears and boundary parallel slip planes (Y) have the same sense of shear as the fault zone, consistent with the deflection of the foliations (S) or synthetic P shears. These deflections indicate that shear strains increase towards the R_1 and Y shears. Antithetic Riedel shears (R_2) and tensile fractures (T) are oriented at large angles to the gouge–host boundary.

*Current address: Shell Internationale Petroleum Mij., Department EPX/32, P.O. Box 162, 2501 AN The Hague, The Netherlands.

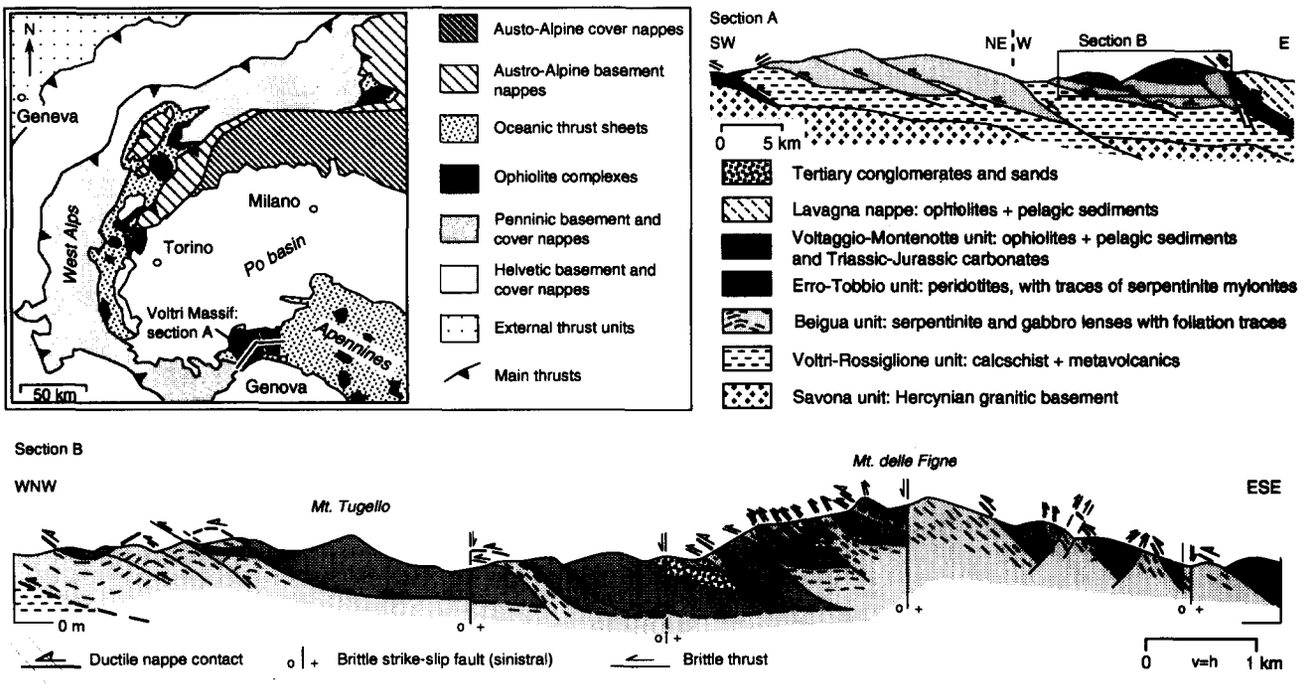

Fig. 2. Simplified tectonic map of the western Alps and northern Apennines. The Austo-Alpine basement and cover nappes are part of the former Apulian continental margin. Fragments of the European passive margin are preserved in the Penninic and Helvetic thrust units. Section A is a schematic profile through the Voltri Massif (see tectonic map for location). Section B shows in greater detail the Alpine thrust structures developed in the eastern part of the Voltri Massif. The studied fault gouges are allied to the brittle thrusts and sinistral strike-slip fault zones dissecting the peridotites of the Erro-Tobbio Unit.

ence the gouge microstructure. On the one extreme, samples deformed at low temperatures and high slip rates show homogeneous deformation and associated development of a pervasive foliation analogous to that in natural clay-rich fault zones. In contrast, samples deformed at lower displacement rates and higher temperatures show distinct localization eventually leading to textures dominated by few discrete shears (*R* and *Y* shears) separating domains of massive gouge.

Despite growing evidence from experimental studies that gouge fabrics dominated by discrete subsidiary shears are closely linked to seismogenic faulting (Dieterich 1981, Sibson 1986, Moore & Byerlee 1991), little attention has as yet focused on natural fault zones showing such extreme localization at the scale of the gouge (e.g. Logan *et al.* 1979, House & Gray 1982, Chester *et al.* 1993). In nature, such gouges have been observed in cataclasites derived from felsic and mafic basement rocks as well as in faulted clay-poor sediments. Below we focus on ultramafic cataclasites developed in serpentinized peridotites from the Voltri Massif, NW Italy (Fig. 2). We investigate the gouge microstructures to infer the dominant deformation mechanisms leading to the development of the gouge. Based on textural analogies with experimental gouges we infer that the brittle faults in the Voltri Massif may represent fossil seismogenic faults dominated by stick–slip sliding. Special attention is paid to frequently observed sigmoidal geometries of the Riedel shears, and a simple geometric relationship is proposed between Riedel shear spacing and the distance between bounding slip planes.

FAULT ZONE STRUCTURES AND GOUGE FABRICS

Geological setting

The Voltri Massif in NW Italy forms part of a series of ophiolite massifs, emplaced in the Alpine suture zone during Eo-Oligocene collision of the African–Apulian and European plates (Fig. 2). The Voltri Massif is made up of a stack of meta-sedimentary, mafic and ultramafic units, separated and transected by brittle thrusts, strike-slip faults and minor normal faults. Early ductile shear zone fabrics in the ultramafic units (Drury *et al.* 1990, Vissers *et al.* 1991, Hoogerduijn Strating & Vissers 1991, Hoogerduijn Strating *et al.* 1993) were partially reactivated and are overprinted by collision-related brittle fault zones. The dominant transport direction was towards the north-northwest, and faulting continued intermittently until at least the Late Miocene (Hoogerduijn Strating *et al.* 1991, Hoogerduijn Strating in press).

Structures in outcrop

The host rocks of the studied brittle faults are massive, slightly serpentinized peridotites of the Erro Tobbio Unit (Fig. 2). The faults are continuous on a scale ranging from a few decimetres to a few kilometres. The larger thrusts and strike-slip faults are characterized by cataclastic zones up to 50 m wide, accommodating displacements of at least several hundreds of metres. Metre-scale duplex structures in the fault zones are common, and early structures in the wall rock such as

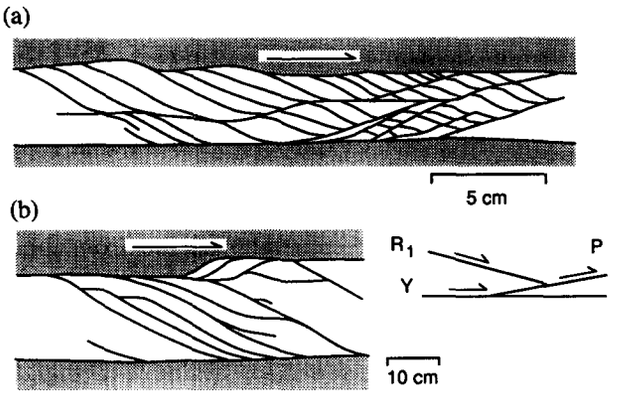

Fig. 3. Different types of serpentinite gouge fabrics observed in the Voltri Massif. (a) Well developed gouge with Y, R_1 and P shears. The upper boundary fault is offset along the R_1 shears. Note sigmoidal shape of the R_1 shears, especially in between the continuous P shears, and the variable spacing of the R_1 shears, changing from about 1 cm on the left side, to about 3 mm in between the P shears. (b) Widely spaced (2–3 cm) R_1 shears bounded by Y shears. Some P shear developed in a left-stepping overlap zone between two Y shears.

foliations and mafic dykes are displaced and locally dragged. The fault surfaces usually are somewhat polished and contain lineations defined by striations and serpentine fibers. In most cases, these lineations are about perpendicular to the intersections of R_1 and Y shears such that they seem reliable indicators of the main shear direction (cf. Tanaka 1992).

Gouges are developed along discrete through-going fault surfaces of highly localized deformation. The gouges consist of centimetre to millimetre-scale angular to subrounded fragments of the wall rock, embedded in a very fine grained, white-weathered matrix. Two planar features are commonly observed: Y shears parallel to the gouge–host rock boundary, and oblique R_1 shears (Figs. 3 and 4a). Some P shears developed and these may form continuous slip planes similar to the P ramps reported by Swanson (1988). However, gouge domains characterized by pervasive foliations are extremely rare. The sense of movement inferred from the orientation of the slip planes with respect to the fault zone margin is consistent with the offset of markers in the wall rock and displacement of fragments in the gouge. Where present, the spacing between the foliation planes is always much smaller than the spacing between any of the slip planes. Commonly, the R_1 and P shears curve asymptotically into the boundary faults, whilst the R_1 shears bend into parallelism with the continuous P shears. The sense of curvature between R_1 and Y shears, and R_1 and P shears is always opposite to the bending of foliations or P shears into the Y shears. The R_1, Y and P shears all have striated surfaces indicative of displacements along these planes. In contrast, there are generally no striations observed on the occasional gouge foliations, suggesting that these foliations are oriented close to the plane of finite flattening.

The angle between the R_1 and Y shears varies between 20° and 35°, with a mean of 25°. It is noted that these angles are larger than the 10–20° commonly observed in clay-rich gouges (e.g. Rutter *et al.* 1986, Chester & Logan 1987, Tanaka 1992) and experimentally deformed serpentinite gouges (Moore *et al.* 1986). The angles also exceed values predicted from theory. For example, in a non-dilational, simple shear fault with a maximum compressive stress oriented at 45° to the fault boundary, a Coulomb–Navier criterion predicts the angle between the Y and R_1 shears to range from 8° in a lizardite-rich gouge (coefficient of internal friction $\mu = 0.3$) to 17° in an antigorite-rich gouge ($\mu = 0.7$; frictional coefficients from Reinen *et al.* 1992a).

The spacing between individual slip planes is not constant (Figs. 3a & b). Instead, from an analysis of a limited number of gouge fabrics it is clear that the spacing between the R_1 shears increases linearly with the distance between bounding Y or P shears, whilst the sub-millimetre spacing between foliation planes in the gouge remains constant. Within the range of observation, the ratio of R_1 vs Y shear spacing is found to be 0.47 (Fig. 6). Notably, in contrast to other studies (Rutter *et al.* 1986, Babaie *et al.* 1991) there is no discernible relationship between clast dimensions in the gouge and shear band spacing.

Microstructures

The peridotite wall rock adjacent to the fault zones consists of partially serpentinized olivine, pyroxene and spinel. Microstructural and petrologic studies (Hoogerduijn Strating & Vissers 1991, Scambelluri *et al.* 1991) have revealed a complex sequence of serpentinite growth in the wall rock preceeding the development of the brittle gouge zones considered in this paper. At the microscale, early, low-temperature static serpentinization is most advanced along pyroxene (100) planes, and along fractures in the olivine grains defining a chrysotile–lizardite mesh texture. These early, static serpentinite fabrics in the wall rock are overprinted by high-temperature, serpentinite shear zones that are characterized by antigorite + magnetite foliations. In the brittle gouge zones discussed here, low-temperature serpentinization is again dominant, both during deformation and as late static overgrowth.

The serpentinite gouge (Fig. 4b) consists of massive microbreccia domains with angular to sub-rounded fragments of serpentinized pyroxene and olivine, embedded in a fine-grained matrix (Fig. 4c). The microbreccia domains are bounded by slip planes defined by bands of aligned serpentine, magnetite and chlorite. In contrast, alignment and elongation of fragments leading to macroscopic foliation development in the microbreccia domains is rare. The pyroxene and olivine grains in the gouge are almost completely replaced by lizardite, chrysotile (identified with X-ray diffraction) and magnetite. Abundant static overgrowth structures suggest that this transformation is essentially post-kinematic. Lizardite in pseudomorphs after pyroxene shows a strong lattice and shape preferred orientation parallel to the original pyroxene (100) planes. Similar pseudomorphs after pyroxene with an oriented lizardite microstructure are also common in undeformed serpentinized peridotite wall rock. The microstructure of the pseudomorphs suggests

that replacement was entirely controlled by the pyroxene lattices. X-ray diffraction analysis of very fine-grained material in the slip planes shows a predominance of low-temperature serpentine minerals (i.e. chrysotile, lizardite), as opposed to the antigorite-rich, high-temperature assemblages preserved in pre-existing shear zone in the wall rock. The chrysotile–lizardite assemblage in the gouge constrains ambient temperatures during brittle deformation to a maximum of around 300°C (Evans 1977). The serpentine mineralogy and mineral chemistry do not provide a pressure constraint, but documented field relations between brittle faulting and deposition of Tertiary scarp breccias (Hoogerduijn Strating *et al.* 1991, Hoogerduijn Strating in press) (see Fig. 2) suggest that confining pressures must have been low (i.e. <1–2 kbar).

The presence of some intact pyroxene grains in the gouge indicates that crack propagation along (partially serpentinized) grain boundaries has been important during fragmentation of the wall rock (see also Hippler & Knipe 1990, Babaie *et al.* 1991). Subsequent fragmentation and grainsize reduction of pyroxenes involved slip along the original (100) planes and preferential microfracturing in areas with a weak to strong undulose extinction. Microfractures are also common close to point contacts between fragments, which indicates that stress concentration and lattice bending were important during the initiation of new transgranular fractures. The dimensions of single crystal olivine fragments in the gouge are approximately equal to the spacing of the serpentine mesh in wall-rock olivine grains (Fig. 7). We therefore suggest that fragmentation of the olivine crystals during cataclasis was largely controlled by crack propagation along olivine grain boundaries and serpentine mesh textures. The strong alteration of the olivine grains in the gouge precludes reliable assessment of how the microstructures evolved during progressive fragmentation. Precursor spinels are preserved in the gouge domains as deformed aggregates of strongly aligned magnetite and chlorite. These grain shape fabrics suggest pre- and/or syn-kinematic transformation of the spinels and, consistent with the lack of any evidence for brittle fracturing, an essentially ductile behaviour of the chlorite–magnetite aggregates.

The gouge material adjacent to the slip planes is completely serpentinized and such domains do not preserve any olivine or pyroxene grains. Instead, foliations may be well developed (Figs. 4d and 5a & b). The foliations are defined by very fine-grained, aligned chrysotile, lizardite, chlorite and extended magnetite aggregates, indicating syn-kinematic growth of this low-temperature mineral assemblage. In addition to the syn-kinematic magnetite in the serpentine foliation, there are euhedral to subhedral magnetite neoblasts adjacent to the slip planes (Fig. 5a) and the slip planes proper are often coated with magnetite (Figs. 4d and 5a & b). Even at the micron scale, backscatter electron microscopy of this magnetite reveals no deformational features, suggesting essentially post-kinematic growth of the magnetite coating and neoblasts. Locally the shear foliations adjacent to Riedel shears are dissected by small slip planes with a synthetic shear sense (Fig. 5b). These subsidiary slip planes most likely developed as secondary synthetic Riedels shears within the primary Riedel structures. The angles between the shear foliations and the slip planes vary from about 30° (Fig. 5a) to less than 8° (Fig. 5b). Assuming non-dilatant simple shear, these angles correspond to shear strains ranging from about 1 to more than 7 (Ramsay & Graham 1970). Syn-kinematic transformation of olivine and pyroxene to serpentine minerals results in a significant volume increase, hence the inferred shear strains only provide a minimum estimate. It follows that considerable displacements must have been accommodated by movement along the discrete slip planes in the gouge. In addition to the major slip planes, which are continuous on the centimetre- to decimetre-scale, there are abundant small discontinuous slip planes. These occur as splays from major displacement zones, generally in R_1 orientations, and as isolated features in the gouge in between major slip planes. Such isolated slip planes are approximately parallel to R_1 or Y shears.

There is no compelling textural evidence for syn-kinematic dilation along the R_1 shears, not even in those sections of the slip planes oriented at a large angle (i.e. >30°) to the Y shears. Moreover, only the presence of small voids adjacent to rotated pyroxene fragments in the gouge reveals that some dilation has occurred adjacent to releasing bends in the slip planes, despite the fact that considerable deformation must have occurred in order to maintain volumetric compatibility. This may suggest that the deformation in the microbreccia domains adjacent to the slip planes has been dominated by grain boundary sliding and grain rotation resulting in some form of bulk cataclastic flow.

Tensile fractures are only observed at the microscopic scale and these are oriented at approximately 45° to the fault zone margins. In the direct vicinity of large pyroxene fragments their orientation may be more irregular, possibly due to local perturbations of the stress field imposed by these fragments. The fractures and small voids adjacent to rotated fragment are filled with fan-shaped aggregates of lizardite and/or chrysotile (Figs. 5c & d). In the fractures, these aggregates tend to nucleate on one side of the fracture leading to an asymmetric fracture fill (Fig. 5c). Whilst asymmetric fracture fill is also observed in other natural fracture systems (e.g. Blenkinsop & Sibson 1992), the reason for the asymmetry is as yet unknown. Sigmoidal tensile fractures and deformed or overprinted fracture arrays are uncommon, which suggests that most tensile fractures were developed at a relatively late stage of gouge formation.

The microscopic observations suggest that fragmentation of the peridotite and serpentine wall rock involved preferential crack propagation along olivine and pyroxene grain boundaries previously weakened during serpentinization. Serpentine mesh textures in olivine have been particularly important in this process. Fragmentation of serpentinized pyroxene grains involved a combination of slip on (100) planes, lattice bending and

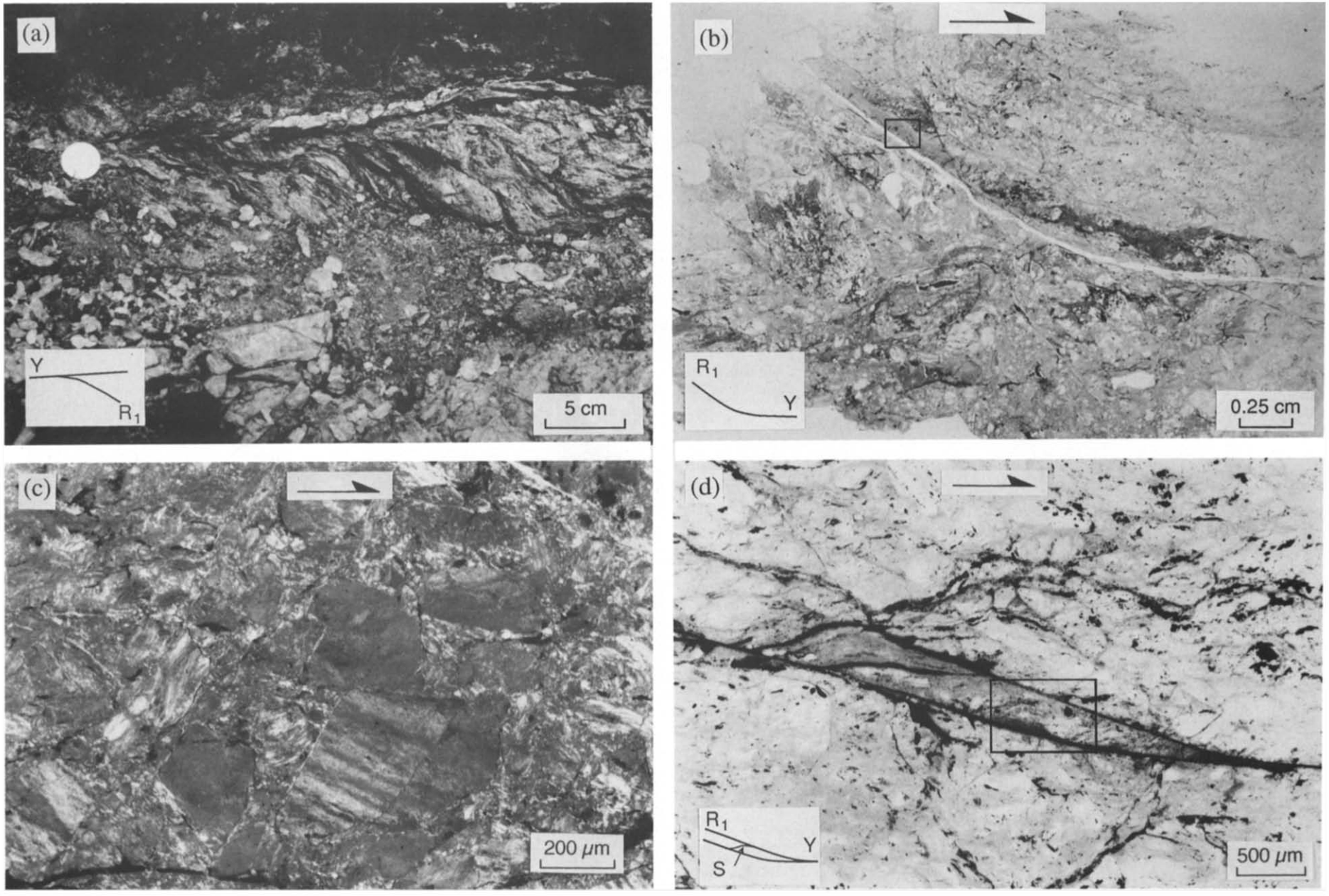

Fig. 4. Photographs of serpentinite gouges. The base of each micrographs is oriented parallel to the Y shears and the sense of shear is right-lateral in all cases. (a) Fault zone with well developed sigmoidal R_1 shears and boundary parallel Y shears bounding lenses of microbreccia. The angle between R_1 and Y shears varies between 25° and 35°. (b) Microbreccia with a R_1 shear bending into a Y shear orientation (thin section is split along the slip plane). The angle between the planar sections of the slip planes is about 32°. The area outlined by the box is shown in Fig. 5(b). (c) Angular fragments of serpentinized pyroxene in a fine-grained matrix of serpentinized olivine (crossed nicols). (d) Gradual transition from R_1 (left) to Y shear (right). The domain in between the R_1 shears is completely serpentinized and a weak foliation developed. The slip planes are coated with magnetite, and a small hexagonal magnetite grain has developed in the foliated domain. The area outlined by the box is shown in Fig. 5(a).

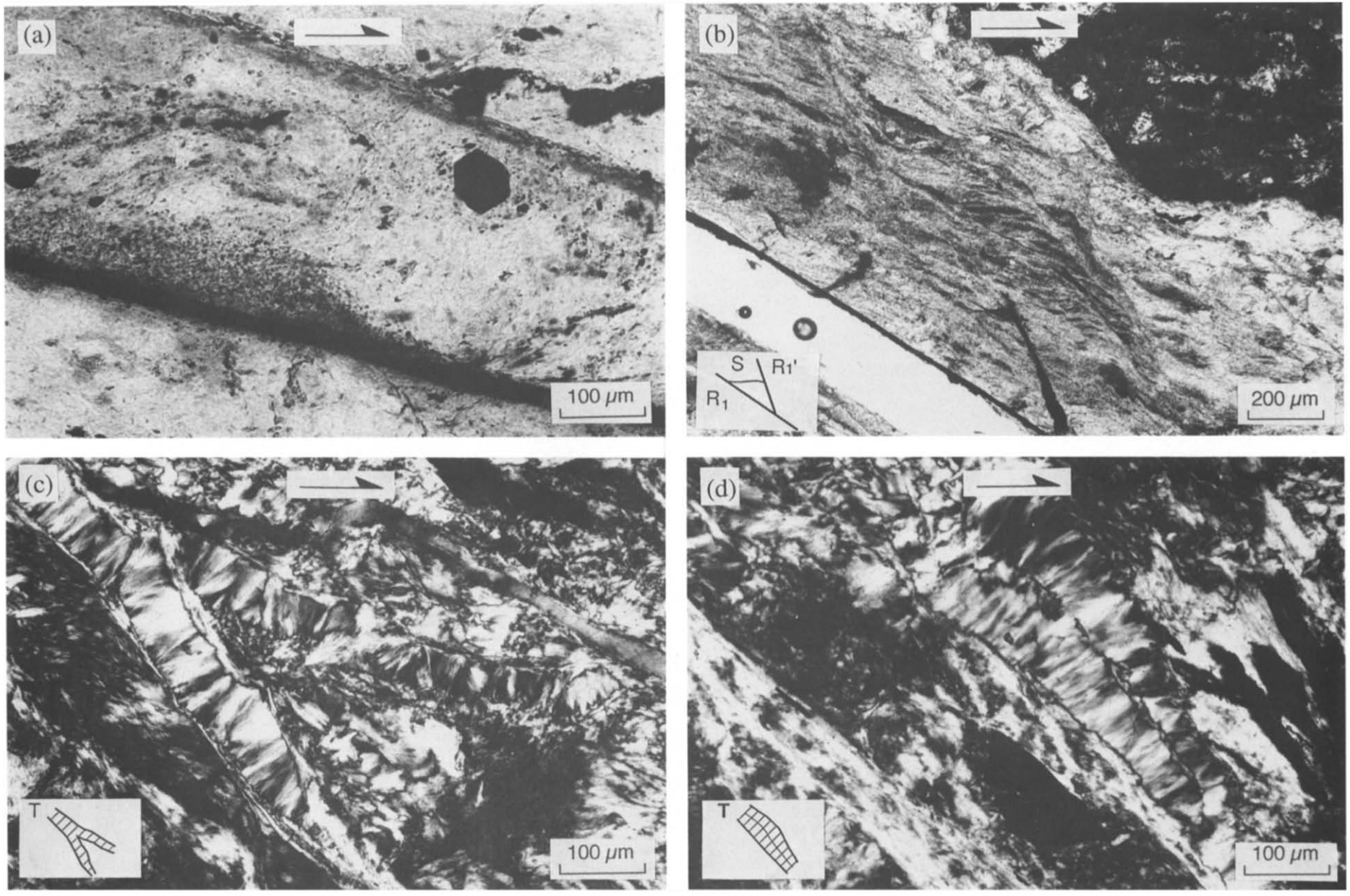

Fig. 5. Microstructures in serpentinite gouges. The base of each micrograph is oriented parallel to the Y shears and the sense of shear is right-lateral in all cases. (a) Detail of Fig. 4(d), showing the alignment of the serpentine minerals defining a vague foliation oriented at approximately 30° to the magnetite coated slip plane, and a post-kinematic hexagonal magnetite grain. (b) Detail of Fig. 4(b), showing well-developed gouge foliation adjacent to a magnetite coated R_1 shear. High-angle dextral shear bands, tentatively interpreted as secondary Riedel shears (R_1'), dissect the foliation. The angle between the shear foliation and the slip plane varies from about 20° to less than 8°. (c) Bifurcating tensile fracture with asymmetric infill of fan-shaped lizardite–chrysotile aggregates (crossed nicols). (d) Tensile fracture with symmetric infill of fan-shaped lizardite–chrysotile aggregates (crossed nicols).

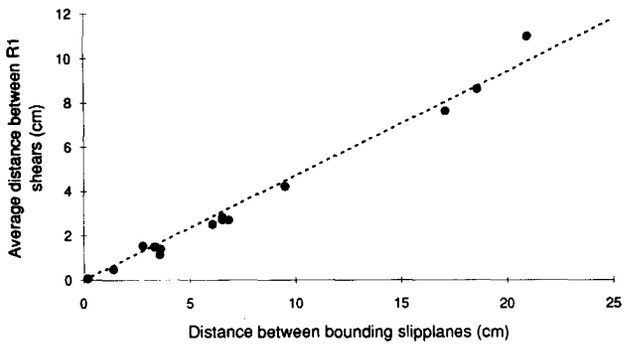

Fig. 6. Relationship between average Riedel separation and distance between bounding Y or P shears. At several locations, characterized by approximately parallel Y or P shears, 5–10 Riedel separations are measured and averaged. All distances are measured perpendicular to the slip planes. The 95% confidence interval corresponds to approximately ±10% of the arithmetic mean. Within the range of observations, the relationship is approximately linear (slope, 0.47; correlation coefficient, $R^2 = 0.98$; number of locations, 13).

transgranular fracturing. At the scale of the gouge, a considerable part of the fault displacement was localized along discrete Y and R_1 shears. Bulk deformation of the microbreccia domains in between these slip planes involved grain boundary sliding, rotation of fragments, and limited movements on small, isolated slip planes. Enhanced serpentinization close to the slip planes indicates that fluids must have been present throughout the deformation history, but the static transformations of the pyroxenes and olivines as well as magnetite coating of the slip planes suggest that serpentinization continued after faulting and cataclastic flow ceased.

DISCUSSION

Because of its relevance to earthquake prediction, there is a strong focus of experimental and theoretical work on the ambient conditions that may be associated with frictional or stable sliding in fault zones (e.g. Logan *et al.* 1979, Dieterich 1981, Ruina 1983, Biegel *et al.* 1989, Chester & Higgs 1992, Linker & Dieterich 1992, Reinen *et al.* 1992b). In general, the development of discrete subsidiary sliding surfaces within the gouge seems to be a necessary condition for frictional instability (Dieterich 1981, Chester *et al.* 1993). Moreover, experiments on sheet silicate gouges including serpentine and illite suggest that the maximum angle between R_1 shears and boundary faults might be indicative of fault sliding behaviour (Moore *et al.* 1989, Moore & Byerlee 1991); i.e. it is inferred that stick–slip faults display a predominance of R_1 shears oriented at relatively large angles to the boundary faults. Experimental serpentinite gouges deformed at 1 kbar confining pressure and displacement rates of 4.8 and 0.048 μm s^{-1} show stable sliding at low temperatures, and stick–slip behaviour at temperatures exceeding approximately 200°C (Moore *et al.* 1983, 1986). On the basis of comparison of the observed microstructures and inferred P–T conditions with experimentally deformed gouges (Higara & Shimamoto 1987, Moore *et al.* 1983, 1986, 1989, Moore & Byerlee 1991) we infer that the brittle faults studied from the Voltri Massif were dominated by stick–slip sliding, and that the Voltri fault zones may represent fossil seismogenic faults. We have not found any pseudotachylytes corroborating this hypothesis. However, it is expected that the inferred high fluid pressures may have inhibited frictional melting (cf. Sibson 1986). On the other hand, it is noted that, in view of the ultramafic compositions involved, any glass quenching from a pseudotachylyte-generated melt would almost instantaneously devitrify to form crystalline products difficult to distinguish from the adjacent ultramafic wall rocks (de Jong personal communication 1993).

Sigmoidal slip planes in fault gouges

The sigmoidal shape of the Riedel shears is a very characteristic but poorly understood feature in many natural and experimental fault gouges. Logan *et al.* (1979) suggested that the curvature might be associated with a decrease of the angle of friction close to the Y shears, because the generally finer-grained material adjacent to the boundary faults would probably be weaker than the coarse-grained gouge material away from the slip planes. The microstructures in the studied serpentinite gouges, however, do not show any appreciable correlation between enhanced grain size reduction close to the boundary faults and Riedel curvature. Therefore, although a gradual increase of the frictional angle away from the Y shears may have contributed to the curvature of the Riedel shears, it does not seem to provide a satisfactory explanation for their curved geometry.

An alternative explanation for the observed sigmoidal shape of the Riedel shears invokes rotation of the slip planes during progressive deformation (cf. Hiraga & Shimamoto 1987). Several studies have shown clear evidence for synthetic or antithetic rotation of R_1 shears (e.g. Riedel 1929, Hempton & Neher 1986, Swanson 1988). Significant synthetic rotation of the R_1 shears in the serpentinite gouges can be ruled out because syn-kinematic dilation has not occurred along the slip planes. Although we cannot exclude a contribution of antithetic rotation, several features suggest that the sigmoidal geometry was initial, and developed during fracture initiation.

(1) Natural as well as experimental fault zones often show half-sigmoidal R_1 shears which curve into a Y or P shear at only one end, whereas the other end terminates in the gouge layer (see also Figs. 3 and 8). Such R_1 fractures must have accommodated extremely limited displacements, inconsistent with any explanation of the curvature near the Y and P shears in terms of progressively accumulated finite strain.

(2) Riedel shears developed in experiments on simulated quartz gouge (Byerlee *et al.* 1978) have been shown to initiate at the boundary faults as small, asymmetric disruption zones. These incipient disruption zones were, most probably, spatially associated with strong regions on the boundary faults (cf. Dieterich 1981). The Riedel

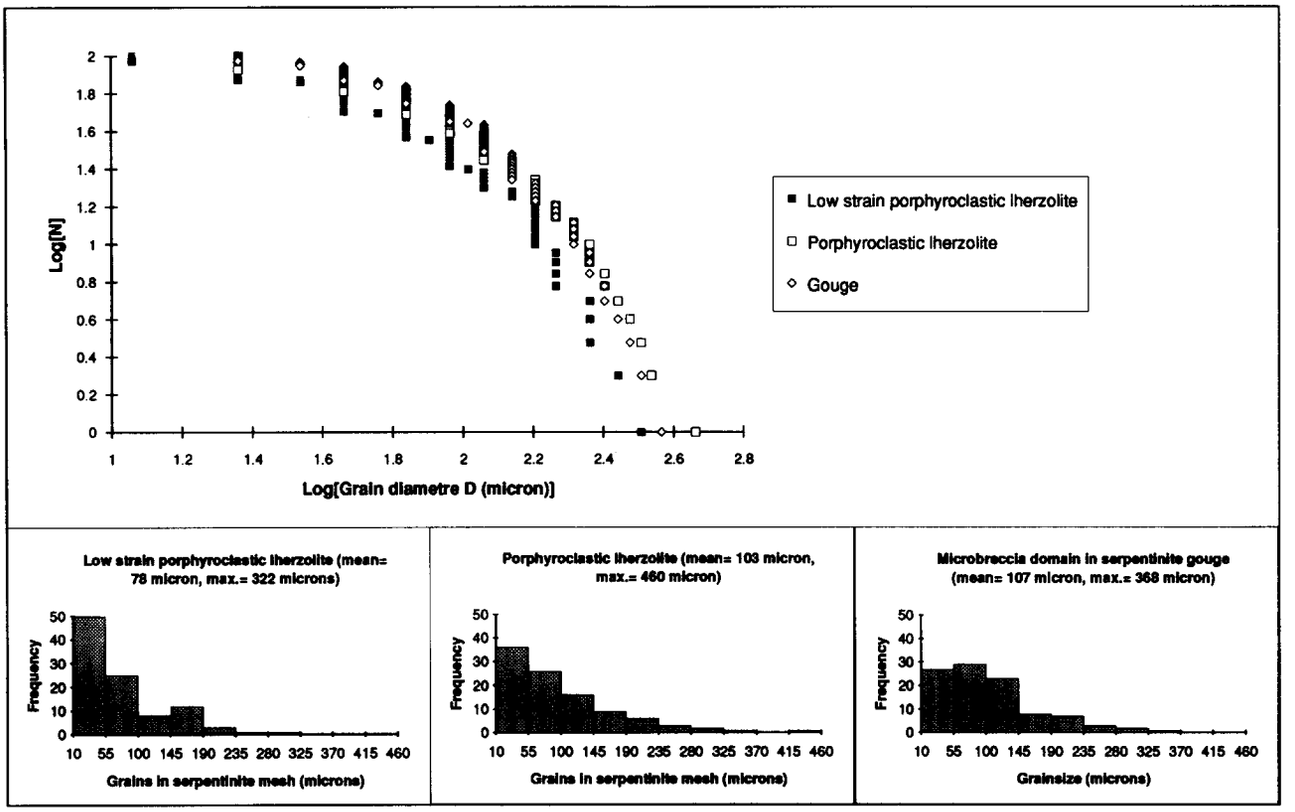

Fig. 7. Size distribution of olivine clasts in a serpentinite gouge, and of olivine fragments bounded by serpentinite mesh in two lherzolite wall rock samples with slightly different initial olivine microstructure and grain size. N is the number of clasts with a diameter greater than D. In each thin section, all grains within a representative area are measured up to a maximum of 100 grains per sample (all measurements at 40 times magnification, smallest grainsize measured 10 μm). The frequency–size distributions are almost identical, suggesting that the olivine grain sizes in the gouge are strongly controlled by the serpentinite mesh texture in the wall rock olivine grains. It is noted that the data are not suited to test the frequency–size distribution on scale-invariant relationships (cf. Biegel *et al.* 1989, Blenkinsop & Sibson 1992).

shears grew progressively from these heterogeneities, until they merged with disruption zones developed at the opposite boundary. For present purposes we emphasize that, even at the earliest stages of fracture growth, the incipient R_1 shears in these experiments tend to curve away gradually from the Y shears.

(3) In addition to the above observations in natural and simulated gouges, we note that isolated Riedel shears (i.e. Riedel shears that do not intersect with Y or P shears) are generally not sigmoidal. This lends support to the hypothesis that the Y or P shears are in some way involved in the development of the sigmoidal geometry.

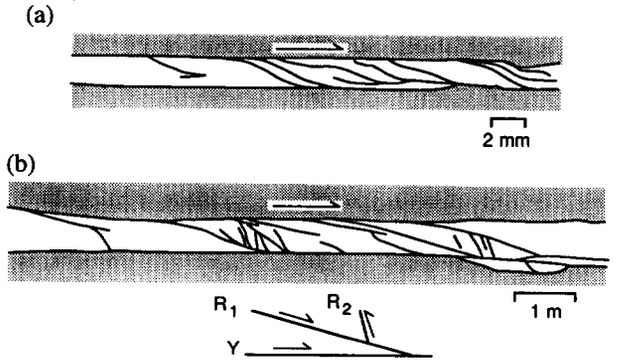

Fig. 8. Line drawings of Riedel shear patterns developed in (a) experimentally deformed simulated quartz gouge (Byerlee *et al.* 1978) and in (b) a segment of the Yorks Cliffs strike-slip fault zone (Swanson 1990). Note the occurrence of both high- and low-angle intersections between R and Y shears. Slightly sigmoidal antithetic Riedel shears are observed in the Yorks Cliff fault. It is suggested that the geometry of these subsidiary faults might be related to the presence or absence of heterogeneities on the boundary faults (see also Fig. 9).

All of these microstructural observations suggest that the sigmoidal geometry of the Riedel shears is not *a priori* related to progressive deformation along existing slip planes, but that it may reflect ambient conditions during fracture initiation. We therefore consider the stress trajectory pattern in a fault zone. Both theoretical (e.g. Chinnery 1966, Segall & Pollard 1980, Bilham & King 1989, Olson & Pollard 1989, Cruikshank *et al.* 1991) and experimental studies (e.g. Freund 1974, Hyett & Hudson 1990, Rawnsley *et al.* 1992) predict that the displacement field (hence the stress field) in the vicinity of an heterogeneity will be disturbed. Based upon the general results of these studies we have drawn schematically the deflection of stress trajectories near three strong points on boundary faults of a non-dilatant simple shear fault zone (Fig. 9). It should be noted that we did not perform a numerical simulation to confirm the exact shape of the trajectories. At the compression side of the heterogeneities, the maximum compressive stress σ_1 will rotate towards the boundary fault. In addition, Mohr–Couloub criteria dictate that the maximum shear stress in the direct vicinity of the strong regions should increase, which favours the initiation of new fractures. Possible traces of Coulomb–Navier shear fractures

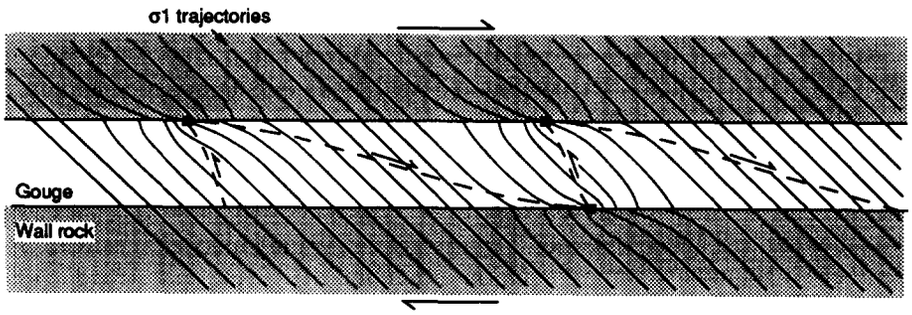

Fig. 9. Schematic representation of the stress trajectories (continuous lines) in a non-dilatant simple shear fault zone containing strong heterogeneities (black squares) on the gouge–wall rock boundary. Consistent with the orientation of the tensile fractures in the gouge, the maximum compressive stress outside the fault zone is assumed to be oriented at 45° to the boundary (see also Mandl *et al.* 1977, Byerlee 1992). Dashed lines indicate traces of possible synthetic and antithetic Riedel shears expected for a Coulomb–Navier failure criterion, assuming a coefficient of internal friction of approximately 0.7 for the gouge material. Note the relatively low intersection angles expected between the boundary faults and subsidiary faults in the direct vicinity of the heterogeneities.

initiating near the heterogeneities are indicated, and it follows that the sigmoidal shape of the R_1 shears can be directly related to such a perturbed stress field. The stress trajectory pattern also suggests that the finite geometry of the Riedel fractures may depend on the presence or absence of strong spots near their intersection with the opposite boundary fault. In case an heterogeneity is present, symmetric sigmoidal fractures with curving low-angle intersections may develop. Otherwise, higher-angle intersections between the two slip planes are anticipated. Examination of natural and experimental fault geometries shows that both high-angle and low-angle curving intersections occur (Figs. 3 and 8).

It is noted that the perturbed stress field of Fig. 9 applies only to the stages prior to initiation of secondary fractures. Upon development of such new fractures, the stress field will modify and this may lead to further complicating fault geometries. We also note that in real fault zones, whether natural or simulated, perturbations of the stress field are to be expected not only near asperities on the boundary faults but also near clusters of relatively rigid fragments derived from the wall rock, or near mechanically weak domains in the gouge (e.g. serpentinite-, chlorite- or clay-rich domains). As a consequence, the orientation of the slip planes near these clusters may vary, and such clusters may act as preferred sites to initiate new fractures (see also Rutter *et al.* 1986). We suggest that the variable orientations of the tensile fractures seen in the serpentinite gouges near pyroxene fragments also reflect perturbations of the bulk stress field.

Another complicating factor in natural fault zones is the role of pore fluids. The pervasive serpentinization and the abundant mineral growth provide ample evidence for the presence of fluids in the studied fault zones. Moreover, both shear fractures and tensile fractures developed in the serpentinite gouges. This suggests that the minimum effective stress has not been constant but that it varied from compressional to tensile. The only mechanically feasible way to allow significant variations of the minimum effective stress during overthrusting (i.e. the effective overburden pressure) involves fluctuations of ambient fluid pressures (Sibson 1986, Chester *et al.* 1993). The growth of fan shaped serpentine aggregates, rather than crack-and-seal fibre textures, indicates that the opening-rate of the tensile fractures exceeded the rate of mineral growth, and that they remained open for time spans long enough to allow the undisturbed growth of the serpentine aggregates. This demonstrates that high fluid pressures persisted in the fault zones in question after development of the tensile fractures. The general lack of evidence for deformation post-dating the formation of the tensile fractures suggests that such high fluid pressures only occurred during the waning stages of overthrusting.

An additional aspect of fluid pressures in fault zones relevant to the geometry of the secondary faults has recently been addressed by Byerlee (1992). It is shown that an increase of the pore pressure reduces the effective frictional coefficient and thus the angle between σ_1 and the Coulomb–Navier shear fractures. However, such an effect probably does not account for the gradual reorientation of subsidiary shears in small-scale fault zones, since it would require considerable fluid pressure gradients to be maintained over short distances within the gouge layer. A 5° decrease of the angle between σ_1 and the shear fracture requires the pore fluid pressure ratio to increase by about 10%. At a depth of 5000 m this implies a relative fluid pressure increase of about 0.1 kbar. Although it may be feasible to have high fluid pressure gradients across permeability barriers like the gouge–wall rock interface (cf. Blanpied *et al.* 1992), it seems problematic in our view to maintain such gradients at a scale of a deforming microbreccia.

R_1 *shear spacing*

The fault rocks from the Voltri Massif show a linear relationship between average Riedel shear spacing and the distance between the bounding slip planes (Fig. 6). Our own observations in some cataclastic fault zones in SW Spain as well as in published experimental gouges (Byerlee *et al.* 1978, Moore *et al.* 1986) and natural fault zones (Chester & Logan 1987, Swanson 1990) indicate that a similar linear relationship may apply to quartz-

dominated gouge zones. The preliminary data suggest that the ratio of R_1 vs Y shear spacing in the quartz-dominated gouges is about 0.44, which is very similar to the value of 0.47 obtained from the serpentinite gouges. We do not fully understand the mechanical explanation for such linear relationships. However, the proportionality between the R_1 and Y or P shear spacings is reminiscent of two other natural fault geometries. (1) In sedimentary rocks there is commonly a linear relationship between bed thickness and joint spacing (e.g. Ladeira & Price 1981, Narr & Suppe 1991). (2) Theoretical models for the development of duplex systems in fold-and-thrust belts suggest a constant thickness–length ratio of horses in a system subjected to constant overburden pressure (i.e. topographic slope $\approx 0°$; Bombolakis 1986). The development of both fracture systems is strongly controlled by (a) the shear stresses acting on, respectively, the bed interface or the floorthrust, and (b) the strength of the material making up, respectively, the competent bed or the horses. If the mechanism controlling the Riedel spacing is indeed somewhat comparable to the mechanisms dictating joint or thrust ramp spacing, it may thus be expected that the Riedel spacing is dependent on the cohesive strength of the gouge material and the shear stresses acting on the bounding Y or P shears. Consequently, the Riedel spacing should be sensitive to the normal stress across the Y or P shears and the rheology of the gouge material: the spacing should theoretically decrease with increasing normal stress or decreasing gouge strength (cf. Ladeira & Price 1981, Bombolakis 1986). Although the number of pertinent observations is as yet very limited, Byerlee *et al.* (1978) reported such a decrease of the Riedel spacing with increasing confining pressure from their experiments on synthetic quartz gouge. Further work is clearly needed to clarify a possible relationship between Riedel spacing, gouge strength and shear stress. Nevertheless, the empirical relation shown in Fig. 6 may be used as a simple geometric rule to discriminate narrowly spaced Riedel shears in natural fault zones from gouge foliations. If the spacing between oblique fabric elements in an outcrop is systematically related to the spacing between bounding slip planes, and the spacing ratio is close to 0.5, the oblique fabric elements are most likely R_1 shear planes. In contrast, the spacing between gouge foliations is fully independent of the distance between Y or P shears, and the spacing ratio will be much smaller than 0.5. This may help to remove some of the ambiguity in the interpretation of brittle fabrics developed in clay-poor gouges, especially if there are no offset markers to confirm the movement sense on the gouge.

CONCLUSIONS

Experimental work on illite and halite gouges indicates that, apart from the composition of the host rock, ambient deformation conditions largely determine whether the deformation in cataclastic fault zones will be homogeneously distributed or extremely localized in few discrete shears. Most natural examples of cataclasites developed in clay-rich compositions are characterized by rather homogeneous deformation in the fault zones. In this paper we described several examples of natural, serpentine-dominated fault zones in which the deformation is extremely localized.

The microstructures indicate that the most important gouge-forming mechanisms were fracturing along (serpentinized) olivine and pyroxene grain boundaries, and initiation of transgranular fractures in domains of lattice bending and stress concentrations near grains contacts. Cataclastic deformation was allied with a marked degree of progressive serpentinization in the fault zones, which added to a mechanical weakening of olivine and pyroxene grains. Textural similarities with experimentally formed gouges suggest that the Voltri fault zones moved by stick–slip sliding; i.e. they may represent fossil seismogenic faults.

The textures in the studied fault zones are dominated by discrete Y and R_1 shears separating domains of more homogenous, massive gouge. Many of the R_1 shears have a clearly sigmoidal shape and gradually curve into Y or P shears. This geometry is inferred to result from perturbations of the stress field near strong heterogeneities on the bounding Y or P shears.

There is a distinct relationship between R_1 shear and Y or P shear spacing, such that the average spacing between the R_1 shears increases linearly with 0.47 times the distance between bounding slip planes. It is suggested that this proportionality may reflect a balance between the cohesive strength of the gouge material and the shear stresses acting on the bounding slip planes. This proportionality provides a simple geometric rule to discriminate, in outcrop, between narrow spaced Riedel shears and gouge foliations. This may help to remove some of that ambiguity in the interpretation of clay-poor natural gouge fabrics.

Acknowledgements—We are indebted for helpful reviews by Diane Moore and Frederick Chester. Comments from Tom Blenkinsop, Susan (Hippler) Haggerty and John Platt helped to clarify some of the topics discussed in this paper.

REFERENCES

Babaie, H. A., Babaei, A. & Hadizadeh, J. 1991. Initiation of cataclastic flow and development of cataclastic foliations in nonporous quartzites from natural fault zones. *Tectonophysics* **200**, 67–77.

Biegel, R. L., Sammis, C. G. & Dieterich, J. H. 1989. The frictional properties of a simulated gouge having a fractal particle distribution. *J. Struct. Geol.* **11**, 827–846.

Bilham, R. & King, G. 1989. The morphology of strike-slip faults: Examples from the San Andreas Fault, California. *J. geophys. Res.* **94**, 10,204–10,216.

Blanpied, M. L., Lockner, D. A. & Byerlee, J. D. 1992. An earthquake mechanism based on rapid sealing of faults. *Nature* **358**, 574–576.

Blenkinsop, T. G. & Sibson, R. H. 1992. Aseismic fracturing and cataclasis involving reaction softening within core material from the Canjon Pass drill hole. *J. geophys. Res.* **97**, 5135–5144.

Bombolakis, E. G. 1986. Thrust–fault mechanics and origin of a frontal ramp. *J. Struct. Geol.* **8**, 281–290.

Byerlee, J. 1992. The change in orientation of subsidiary shears near faults containing pore fluid under high pressure. *Tectonophysics* **211**, 295–303.

Byerlee, J., Mjachkin, V., Summers, R. & Voevoda, O. 1978. Struc-

tures developed in fault gouge during stable sliding and stick–slip. *Tectonophysics* **44**, 161–171.
Chester, F. M., Friedman, M. & Logan, J. M. 1985. Foliated cataclasites. *Tectonophysics* **111**, 139–146.
Chester, F. M. & Logan, J. M. 1987. Composite planar fabric of gouge from the Punchbowl Fault, California. *J. Struct. Geol.* **9**, 621–634.
Chester, F. M. & Higgs, N. G. 1992. Multimechanism friction constitutive model for ultrafine quartz gouge at hypocentral conditions. *J. geophys. Res.* **97**, 1859–1870.
Chester, F. M., Evans, J. P. & Biegel, R. L. 1993. Internal structure and weakening mechanisms of the San Andreas Fault. *J. geophys. Res.* **98**, 771–786.
Chinnery, M. A. 1966. Secondary faulting. I. Theoretical aspects. *Can. J. Earth Sci.* **3**, 163–190.
Cruikshank, K. M., Zhao, G. & Johnson, A. M. 1991. Analysis of minor fractures associated with joints and faulted joints. *J. Struct. Geol.* **13**, 865–886.
Dieterich, J. H. 1981. Constitutive properties of faults with simulated gouge. *Am. Geophys. Un. Geophys. Monogr.* **24**, 103–120.
Drury, M. R., Hoogerduijn Strating, E. H. & Vissers, R. L. M. 1990. Shear zone structures and microstructures in mantle peridotites from the Voltri Massif, Ligurian Alps, N.W. Italy. *Geologie Mijnb.* **69**, 3–17.
Evans, B. W. 1977. Metamorphism of alpine peridotite and serpentinite. *Annu. Rev. Earth & Planet Sci.* **5**, 397–447.
Evans, J. P. 1988. Deformation mechanisms in granitic rocks at shallow crustal levels. *J. Struct. Geol.* **10**, 437–443.
Evans, J. P. 1990. Textures, deformation mechanisms and the role of fluids in the cataclastic deformation of granitic rocks. *Spec. Publs geol. Soc. Lond.* **54**, 29–39.
Freund, E. 1974. Kinematics of transform and transcurrent faults. *Tectonophysics* **21**, 93–143.
Hempton, M. R. & Neher, K. 1986. Experimental fracture, strain and subsidence patterns over en échelon strike-slip faults: implications for the structural evolution of pull-apart basins. *J. Struct. Geol.* **8**, 597–605.
Hippler, S. J. & Knipe, R. J. 1990. The evolution of cataclastic fault rocks from a pre-existing mylonite. In: Deformation Mechanisms, Rheology and Tectonics (edited by Knipe, R. J. & Rutter, E. H.). *Spec. Publs geol. Soc. Lond.* **54**, 71–79.
Hoogerduijn Strating, E. H. In press. Extensional faulting in an intraoceanic subduction complex—A working hypothesis for the Paleogene of the Alps–Apennine system. *Tectonophysics*.
Hoogerduijn Strating, E. H., Rampone, E., Piccardo, G. B., Drury, M. R. & Vissers, R. L. M. 1993. Subsolidus emplacement of mantle peridotites during incipient oceanic rifting and opening of the Mesozoic Tethys (Voltri Massif, NW Italy). *J. Petrol.* **34**, 901–927.
Hoogerduijn Strating, E. H., Van Wamel, W. A. & Vissers, R. L. M. 1991. Some constraints on the kinematics of the Tertiary Piemonte Basin. *Tectonophysics* **198**, 47–51.
Hoogerduijn Strating, E. H. & Vissers, R. L. M. 1991. Dehydration-induced fracturing of eclogite facies peridotites: implications for the mechanical behaviour of subducting oceanic lithosphere. *Tectonophysics* **200**, 187–198.
House, W. M. & Gray, D. R. 1982. Cataclasites along the Saltville thrust, U.S.A., and their implications for thrust sheet emplacement. *J. Struct. Geol.* **4**, 257–269.
Hiraga, H. & Shimamoto, T. 1987. Textures of sheared halite and their implications for the seismogenic slip of deep faults. *Tectonophysics* **144**, 69–86.
Hyett, A. I. & Hudson, J. A. 1990. A photo-elastic investigation of the stress state close to rock joints. In: *Rock Joints* (edited by Barton, N. & Stephansson, O.). Balkema, Rotterdam, 227–233.
Ladeira, F. L. & Price, N. L. 1981. Relationship between fracture spacing and bed thickness. *J. Struct. Geol.* **3**, 179–184.
Linker, M. F. & Dieterich, J. H. 1992. Effects of variable normal stress on rock friction: Observations and constitutive equations. *J. geophys. Res.* **97**, 4923–4940.
Logan, J. M., Friedman, M., Higgs, N. G., Dengo, C. & Shimamoto, T. 1979. Experimental studies of simulated gouge and their application to studies of natural fault zones. *U.S. geol. Surv. Open-file Rep.* **79-1239**, 305–343.
Logan, J. M. & Rauenzahn, K. A. 1987. Frictional dependence of gouge mixtures of quartz and montmorillonite on velocity, composition and fabric. *Tectonophysics* **144**, 87–108.
Mandl G., De Jong, N. J. & Maltha A. 1977. Shear zones in granular material: an experimental study of their structure and mechanical genesis. *Rock Mech.* **9**, 95–144.
Moore, D. E. & Byerlee, J. 1991. Comparative geometry of the San Andreas fault, California, and laboratory fault zones. *Bull. geol. Soc. Am.* **103**, 762–774.
Moore, D. E., Summers, R. & Byerlee, J. D. 1983. Strength of clay and non-clay fault gouges at elevated temperatures and pressures. *Proc. U.S. Symp. Rock Mechanics* **24**, 489–500.
Moore, D. E., Summers, R. & Byerlee, J. D. 1986. The effect of sliding velocity on the frictional and physical properties of heated fault gouge, behaviour and deformation textures of heated illite gouge. *Pure & Appl. Geophys.* **124**, 31–52.
Moore, D. E., Summers, R. & Byerlee, J. D. 1989. Sliding behaviour and deformation textures of heated illite gouge. *J. Struct. Geol.* **11**, 329–342.
Narr, W. & Suppe, J. 1991. Joint spacing in sedimentary rocks. *J. Struct. Geol.* **13**, 1037–1048.
Olson, J. & Pollard, D. D. 1989. Inferring paleostresses from natural fracture patterns: A new method. *Geology* **17**, 345–348.
Power, W. C. & Tullis, T. E. 1989. The relationship between slickenside surfaces in fine-grained quartz and the seismic cycle. *J. Struct. Geol.* **7**, 879–893.
Ramsay, J. G. & Graham, R. H. 1970. Strain variations in shear belts. *Can. J. Earth Sci.* **7**, 786–813.
Rawnsley, K. D., Rives, T., Petit, J.-P., Hencher, S. D. & Lumsden, A. C. 1992. Joint development in perturbed stress field near faults. *J. Struct. Geol.* **14**, 939–951.
Reinen, L. A., Weeks, J. D. & Tullis, T. E. 1992a. Comparison of the frictional constitutive behaviour of antigorite and lizardite serpentine polymorphs. *Eos* **73**, Fall Meeting Suppl., 511.
Reinen, L. A., Tullis, T. E. & Weeks, J. D. 1992b. Two-mechanism model for frictional sliding of serpentinite. *Geophys. Res. Lett.* **19**, 1535–1538.
Ruina, A. L. 1983. Slip instability and state variable friction laws. *J. geophys. Res.* **91**, 521–530.
Riedel, W. 1929. Zur mechanik geologischer Brucherscheinungen. *Zbl. Mineral. Geol. Palaeont., Abt.* **1929B**, 354–368.
Rutter, E. H., Maddock, R. H., Hall, S. H. & White, S. H. 1986. Comparative microstructures of natural and experimentally produced clay-bearing fault gouges. *Pure & Appl. Geophys.* **124**, 3–30.
Scambelluri, M., Hoogerduijn Strating, E. H., Piccardo, G. B., Vissers, R. L. M. & Rampone, E. 1991. Alpine olivine- and titanian clinohumite-bearing assemblages in the Erro-Tobbio peridotite (Voltri Massif, NW Italy). *J. metamorph. Geol.* **9**, 79–91.
Segall, P. & Pollard, D. D. 1980. Mechanics of discontinuous faults. *J. geophys. Res.* **85**, 4337–4350.
Sibson, R. H. 1986. Earthquakes and rock deformation in crustal fault zones. *Annu. Rev. Earth Planet. Sci.* **14**, 149–175.
Skempton, A. W. 1966. Some observations on tectonic shear zones. *Proc. Int. Congr. Rock Mechanics* **1**, 329–335.
Swanson, M. T. 1988. Pseudotachylyte-bearing strike-slip duplex structures in the Fort Foster Brittle Zone, S. Maine. *J. Struct. Geol.* **10**, 813–828.
Swanson, M. T. 1990. Extensional duplexing in the York Cliffs strike slip fault system, southern coastal Maine. *J. Struct. Geol.* **12**, 499–512.
Tanaka, H. 1992. Cataclastic lineations. *J. Struct. Geol.* **14**, 1239–1252.
Tchalenko, J. S. 1970. Similarities between shear zones of different magnitudes. *Bull. geol. Soc. Am.* **81**, 1625–1640.
Vissers, R. L. M., Drury, M. R., Hoogerduijn Strating, E. H. & van der Wal, D. 1991. Shear zones in the upper mantle: A case study in an Alpine lherzolite massif. *Geology* **19**, 990–993.